NEOPLASIA
www.neoplasia.com

Volume 10 Number 4 April 2008 pp. 371–379 371

An *In Vivo* Mouse Model for Human Prostate Cancer Metastasis[1,2,3]

Aaron M. Havens*,†, Elisabeth A. Pedersen*, Yusuke Shiozawa*, Chi Ying‡, Younghun Jung*, Yanxi Sun*,§, Chris Neeley‡, Jincheng Wang*, Rohit Mehra‡, Evan T. Keller‖, Laurie K. McCauley*,¶, Robert D. Loberg‡, Kenneth J. Pienta‡ and Russell S. Taichman*

*Department of Periodontics and Oral Medicine, University of Michigan School of Dentistry, Ann Arbor, MI 48109, USA; †Harvard School of Dental Medicine, 188 Longwood Ave, Boston, MA, 02115, USA; ‡Department of Internal Medicine, Division of Hematology/Oncology, University of Michigan School of Medicine, Ann Arbor, MI, 48109, USA; §Department of Ophthalmology, Nanjing Tongren Hospital, Nanjing, Jiangsu Province, China; ‖Department of Urology, University of Michigan, Ann Arbor, MI 48109, USA; ¶Department of Pathology, University of Michigan School of Medicine, Ann Arbor, MI 48109, USA

Abstract

We developed a sensitive real-time polymerase chain reaction (*Q*PCR) assay that allows us to track early lodging/homing events *in vivo.* We used this technology to develop a metastasis assay of human prostate cancer (PCa) growth in severe combined immunodeficient mice. For this purpose, marked human PCa cell lines were implanted subcutaneously or in the prostate (orthotopically) of severe combined immunodeficient mice as models of primary tumors. Mice were then sacrificed at various time points, and distant tissues were investigated for the presence of metastatic cells. At 3 weeks, a number of tissues were recovered and evaluated by *Q*PCR for the presence of metastatic cells. The data demonstrate that several PCa cell lines are able to spread from the primary lesion and take up residence in distant sites. If the primary tumors were resected at 3 weeks, in several cases, metastastic lesions were identified over the course of 9 months. We propose that this new model may be particularly useful in exploring the molecular events in early metastasis, identifying the metastatic niche, and studying issues pertaining to dormancy.

Neoplasia (2008) 10, 371–379

Introduction

The metastatic spread of cancer cells is a dreaded complication of malignant neoplasms. Metastasis is a multistep process in which malignant cells must initially *escape* from the primary tumor, invade the surrounding tissues, and enter the vascular circulation [1]. If they are able to survive in the blood stream, they must successfully arrest at a secondary target site, cross the vascular barrier, and migrate into the extravascular connective tissues. Subsequently, tumor cells may proliferate to form a clinically relevant metastatic colony. Alternatively, they may remain dormant, potentially never proliferating beyond a microscopic focus of cells. The molecular bases of metastasis and, particularly, dormancy are poorly understood.

Having a primary tumor as a source of cancer cells is clearly a prerequisite for establishing metastases. It is also clear that primary

Address all correspondence to: Russell S. Taichman, Department of Periodontics and Oral Medicine, University of Michigan School of Dentistry, 1011 North University Avenue, Ann Arbor, MI 48109-1078. E-mail: rtaich@umich.edu

[1]This work was directly supported by the Charles Eliot Ware Memorial Fellowship (A.M. Havens), Pediatric Oncology Research Fellowship (Y. Shiozawa), CA93900 (L.K. McCauley, E.T. Keller, K.J. Pienta, and R.S. Taichman), the Department of Defense PC060857 (R.S. Taichman), P50 CA69568 (K.J. Pienta), U19 CA113317 (K.J. Pienta), and 2006 and 2007 awards from the Prostate Cancer Foundation (R.S. Taichman and K.J. Pienta). K.J. Pienta receives support as an American Cancer Society Clinical Research Professor.

[2]This work is dedicated to Leslie Taichman. May she heal quickly.

[3]This article refers to a supplementary material, which is designated by Figure W1 and is available online at www.neoplasia.com.

Received 13 January 2008; Revised 29 January 2008; Accepted 30 January 2008

 1522-8002/08/$25.00
DOI 10.1593/neo.08154

tumors affect the host systemically, possibly *priming* distant tissues, creating premetastatic niches that are conducive for tumor seeding [2–4]. This may influence both the seeding rate and/or growth of secondary tumors. It may also precondition selective sites for the distinct metastatic patterns as described by Paget [5] in the original *seed-and-soil* hypothesis. Yet, to study each of these possibilities and, in particular, early metastatic events, a model system must be in place, which recapitulates what is observed clinically. Unfortunately, the number of experimental systems of spontaneous metastasis using human prostate cancer (PCa) cell lines is limited. Moreover, common systems used to explore metastasis bypass many of the early steps in the process, particularly when the tumor cells are placed directly into the circulation.

To approach this problem, we developed a sensitive real-time polymerase chain reaction (*Q*PCR) assay that allows us to track early lodging/homing events *in vivo*. We used this technology to develop a metastasis assay of human PCa growth in severe combined immunodeficient (SCID) mice. For this purpose, marked human PCa cell lines were implanted subcutaneously (s.c.) or in the prostate (orthotopically) in SCID mice as models of primary tumors. Mice were then sacrificed at various time points, and distant tissues were investigated for the presence of metastatic cells. At 3 weeks, a number of tissues were recovered and evaluated by *Q*PCR for the presence of metastatic cells. These data demonstrate that several PCa cell lines are able to spread from the primary lesion and take up residence in distant sites. If the primary tumors were resected at 3 weeks, in several cases, metastastic lesions were identified over the course of 9 months. We propose that this new model may be particularly useful in exploring the molecular events in early metastasis, identifying the metastatic niche, and studying issues pertaining to dormancy. The model is highly adaptable and amenable to experimental manipulation, and as such, the model will clearly be useful to the scientific community in identifying the molecular mechanisms of metastatic PCa disease.

Materials and Methods

Cell Lines

LNCaP cells are androgen-responsive, nonmetastatic, and produce mildly osteoblastic lesions when injected into the bone. C4-2B cells were derived through serial passages of LNCaP cells in mice [6]. LNCaP C4-2B cells, kindly provided by Dr. L. Chung (Emory University), are androgen-independent, metastasize to bone, and form mixed osteoblastic/osteolytic lesions. PC-3 cells are androgen-independent, highly metastatic, and produce very osteolytic lesions. PC-3 and LNCaP C4-2B cells expressing a pLazarus retroviral construct containing luciferase were selected as described [7]. All cell lines were cultured in RPMI 1640 containing 10% FBS and antibiotics and maintained at 37°C, 5% CO_2, and 100% humidity.

Animal Manipulations

Male 5- to 7-week-old SCID mice (CB.17. SCID; Taconic, Germantown, NY), used as transplant recipients, were housed under constant humidity and temperature, with 12-hour light/12-hour dark cycles, and monitored daily. The animals were anesthetized by isoflurane inhalation. Each group consisted of a range of 8 to 10 animals. On achieving the endpoints of the study, the animals were anesthetized, and phlebotomy was performed by intracardiac puncture. The animals were then sacrificed, and tissue samples were dissected free from the surrounding tissues (the original scaffold, calvaria, brain, tongue, mandible, heart, lung, kidney, adrenal gland, liver, periaortic lymph nodes, prostate, tibia, humeri, femur, spleen, pelvis, spine, fat, eye, and blood). Tissues were snap-frozen and stored at −80°C until DNA extraction. DNA was extracted from the animals' left organ/tissue where applicable, with the following exceptions: the left lower lobe of the lung and the left lobe of the liver. Extraction of DNA from the entire brain, heart, and tongue was also performed.

Implantation of Scaffolds Containing PCa Cell Lines

Sterile collagen scaffolds (3 × 3 × 3 mm^3, Gelfoam; Pharmacia & Upjohn Co., New York, NY) were used for the transplantation of human PCa cells. Immediately before transplantation, 2×10^5 PCa cells were resuspended in 20 μl of RPMI 1640 containing 5% FBS and antibiotics and were allowed to adsorb into the scaffolds. A single mid dorsal incision was made for the implantation of the tumor-bearing scaffolds and was closed with surgical clips. The animals were monitored daily, and tumor volumes were calculated using the following formula: V = (the shortest diameter)^2 × (the longest diameter) at 21 days.

Tumor Initiation By Orthotopic Route

After anesthesia with ketamine (50 mg/kg) and xylazine (10 mg/kg), a low midline incision was made in the lower abdomen. PCa cells (2×10^5 in 20 μl of PBS) were injected into the right or left dorsolateral lobe of the prostate, and the wound was closed with surgical clips [8].

Vertebral Body Transplant (Vossicle) Implantation

Lumbar vertebrae were isolated from the C57/Bl6 mice (Jackson Laboratory, Bar Harbor, ME) within 4 days of birth. Soft tissues were dissected, and the vertebrae were sectioned into single vertebral bodies (vossicles) with a scalpel blade. Male 5- to 7-week-old SCID mice, used as transplant recipients, were anesthetized with isoflurane inhalation. Two 1-cm incisions were made along the back of each mouse. Pouches made on either side of the incision by blunt dissection were implanted. Four vossicles were implanted in the dorsal region of each mouse (n = 4). The surgical sites were closed with surgical clips.

Bioluminescence

Mice were injected intraperitoneally with luciferin (100 μl at 40 mg/ml in PBS) before imaging. This dose and route of administration have been shown to be optimal for rodent studies with a 10- to 20-minute post–luciferin injection [9]. Mice were anesthetized, and a cryogenically cooled imaging system (IVIS Imaging System; Xenogen, Mountain View, CA) was used for data acquisition [10]. Whole animal imaging was used to monitor tumor growth. Signal intensities were quantified as the sum of all detected photons (Figure W1).

Real-Time Polymerase Chain Reaction

DNA isolaton kits were used to prepare genomic DNA from the designated tissues (DNeasy Blood and Tissue Kit (Cat. no. 69506); Qiagen, Inc., Valencia, CA). DNA extraction was preformed directly according to the Qiagen protocol. All sample concentrations were standardized in each reaction to exclude false-positive results. Real-time polymerase chain reactions were preformed using 15.0 μl of TaqMan PCR Master Mix (Applied Biosystems, Foster City, CA) with

100 nM of the *Luc* [TaqMan probes (F – 5′-CGG CTG GCA GAA GCT ATG AA, R – 5′-TCG CTG CAC ACC ACG AT, TaqMan probe – 5′-FAM-CTA TGG GCT GAA TAC AAA CC) or human *Alu* TaqMan probes (F – 5′-CAT GGT GAA ACC CCG TCT CTA-3′, R – 5′-GCC TCA GCC TCC CGA GTA G-3′, TaqMan probe – 5′-FAM-ATT AGC CGG GCG TGG TGG CG-TAMRA-3′); Applied Biosystems] [11] and 1 μg of the isolated tissue DNA in a total volume of 30 μl. The thermal conditions were 50°C for 2 minutes, 95°C for 10 minutes followed by 40 cycles of 95°C for 15 seconds and 60°C for 1 minute. The level of expression was detected as an increase in fluorescence using a sequence detection system (ABI PRISM 7700; Applied Biosystems). The DNA levels were expressed as relative copies (% control) normalized against murine *β-actin* (Cat. no. 4331182; Applied Biosystems), and a standard curve constructed from serial dilutions of a purified *Luc*/*Alu* cDNA fragment was cloned by classic PCR. Numerical data were determined against a standard curve established using murine bone marrow containing log-fold dilutions of human PCa cells. Positive and negative controls include tissues obtained from non–PCa-injected mice or DNA derived directly from PCa cells.

Parathyroid Hormone Injections

Mice were administered recombinant human parathyroid hormone (1–34) (Bachem, Torrance, CA) or vehicle (0.9% saline) by subcutaneous injection at 40 μg/kg per day for 3 weeks. Animals were weighed weekly, and the dosage was adjusted accordingly [12].

Intravital Microscopy

Multiphoton imaging consisted of a modified confocal microscope system (FluoView 300; Olympus, Center Valley, PA) coupled to a Mai Tai Broadband, Mode-Locked Ti:sapphire Laser (Spectra-Physics, Mountain View, CA) femtosecond-pulsed and tunable between 700 and 990 nm. A total of 2×10^5 PC-3 cells expressing green fluorescent protein were implanted s.c. in SCID mice. At 3 weeks, 10 to 20 μl of 2 μM Qtracker 655-nm nontargeted quantum dots (Quantum Dot Corporation, Hayward, CA) diluted in a total of 100 μl of PBS was injected into the lateral tail vein to nonspecifically label vascular network surrounding the resulting tumors. After 20 to 30 minutes, animals were anesthetized through intraperitoneal injection of ketamine/xylazine. The skin was retracted laterally from the incision, and a custom-made poly(dimethylsiloxane) viewing chamber was placed in contact with the exposed skin. The chambers were filled with PBS during the microscope observation lasting 30 to 90 minutes.

Immunohistochemistry

The formalin-fixed, decalcified, and paraffin-embedded tissues were dewaxed and placed in a pressure cooker containing 0.01-M buffered sodium citrate solution (pH 6.0), boiled, and chilled to room temperature for antigen retrieval. Murine tissues were harvested and fixed in 10% neutral-buffered formalin (Sigma, St. Louis, MO) overnight. The long bones were decalcified in 10% EDTA, pH 7.5, for 14 days at 4°C. In addition, 7-μM paraffin-embedded slides were prepared, stained with 20-μg/ml rabbit polyclonal to luciferase antibody (Abcam Inc. Cambridge, MA) or an IgG (Sigma) in conjunction with an HRP-AEC staining kit following the manufacturers' protocols (R&D Systems, Minneapolis, MN). Images were taken by a microscope (Eclipse E800; Nikon, Melville, NY), with objective 40× NA 0.76, and a camera (RT Slider; Diagnostic Instruments, Sterling Heights, MI) and were analyzed using a software (Image-Pro Plus version 5.1.2.59; Media Cybernetics, Inc., Bethesda, MD).

Statistical Analysis

Numerical data are expressed as means ± SD. Statistical differences between the means for the different groups were evaluated with Instat 4.0 (GraphPad software, San Diego, CA) using one-way analysis of variance (ANOVA) with the level of significance at $P < .05$. Unless indicated, Kruskal-Wallis test and Dunn's multiple comparisons tests were used with the level of significance set at $P < .05$.

Results

Dissemination Patterns of Human PCa Cell Lines in SCID Mice

The prostate cancer field is critically lacking a metastasis assay in which human tumor cells can be implanted *in vivo* and all the steps of metastasis, including vascular invasion and egress, are achieved. In recent studies, we developed an extremely sensitive *Q*PCR assay that allows us to track lodging/early homing events of hematopoietic stem cells. We therefore evaluated whether this technology could be used to develop a metastasis assay of human PCa growth in SCID animals. For this purpose, 2×10^5 PC-3^{luciferase} or LNCaP C4-2B cells were initially implanted s.c. in sponges on the backs of SCID mice (e.g., a primary tumor). At 3 weeks, a number of tissues were recovered and evaluated for either human *Alu* sequences or luciferase by *Q*PCR to detect the presence of the human metastatic cells when the tumors had reached an average of ~209 ± 16.4 and ~157 ± 12.3 mm^2 for the PC-3 and LNCaP C4-2B tumors, respectively. To establish cell numbers, standard curves were generated using whole murine bone marrow seeded with known numbers of human PCa cell lines (data not presented).

As shown in Figure 1, s.c. implantation of PC-3 and LNCaP C4-2B cells resulted in a significant number of shed or *metastatic* cells in a variety of tissues. In animals that were not implanted with human PCa, no *Alu* or *luciferase* signals were observed. LNCaP C4-2B cell levels were generally higher than PC-3 levels in the soft tissues evaluated, although no consistent pattern was noted for the distribution. In osseous tissues, PC-3 cell levels were highest in the calvaria, femur, and humeri, whereas LNCaP C4-2B levels were higher in the spine and tibia (Figure 1).

Disseminated Human PCa Cells Are Able to Form Tumors

The preceding results suggest that human PCa cells are able leave the primary tumor and disseminate to distant organs. As an alternative explanation, genetic material shed from the human cells was identified by PCR in the murine tissues. As an initial attempt to distinguish between these possibilities, two separate studies were performed. In the first, a multiphoton imaging system was used to examine in real-time the localization of PCa cells and stromal components in tissues up to 1 mm in depth. PC-3 cells expressing green fluorescent protein were grown s.c. in SCID mice. The animals were then injected with nontargeted quantum dot 605-nm solution to label the blood vessels. To determine if the human PCa cells were able to egress from the primary tumor, a ~0.5-cm incision was made in the skin on one side of the tumor in a crescent shape, and the tumor-bearing skin flap was externalized and viewed. Figure 2*A* demonstrates a fairly compact tumor

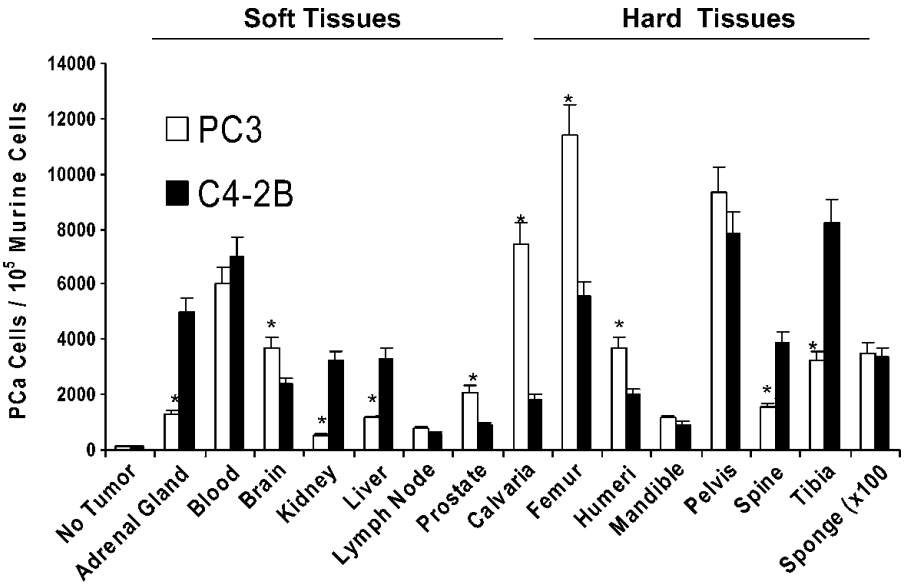

Figure 1. Development of a metastasis assay for human PCa. Luciferase-labeled PC-3 or LNCaP C4-2B cells (2×10^5 cells) were implanted s.c. in sponges on the backs of SCID mice ($n = 10$) as a primary tumor model. At 3 weeks, the animals were sacrificed, and tissues were removed. *Q*PCR was used to detect human *Alu* sequences (shown) or luciferase (not shown) derived from the human PCa cells. Pilot studies, not shown, demonstrated a ~1:1 correlation between *Q*PCR tracking of human *Alu* and luciferase sequences. Resultant numbers were generated against a standard curve established by mixing known numbers of PC-3 or C4-2B cells in mouse marrow. Further normalization was performed for differences in mouse tissue density using murine *β-actin* primers. Human *Alu* was not identified in animals not receiving a s.c. tumor (No Tumor). *Significance difference of PC-3 *versus* C4-2-B ($P < .05$). Data show that shed or metastatic PCa cells can be identified in a number of tissues derived from s.c. tumors.

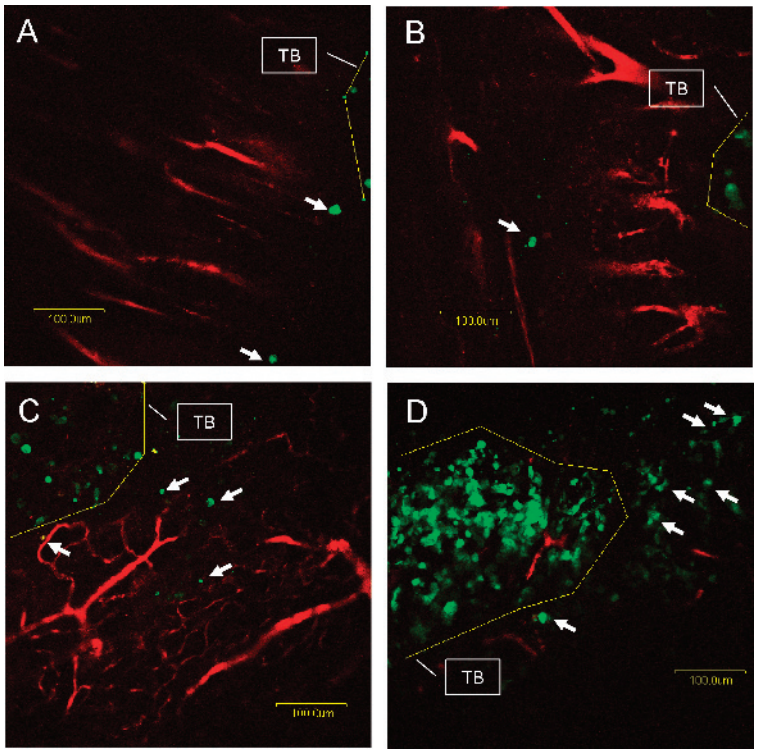

Figure 2. Multiphoton imaging of initial tumor dissemination. A multiphoton imaging system was used to examine in real-time the localization of PCa cells and stromal components in tissues. PC-3 cells expressing green fluorescent protein were grown s.c. in SCID mice. At 3 weeks, the animals were injected with a nontargeted quantum dot (605 nm) to label the blood vessels (Red). Thirty minutes later, tumor-bearing skin flaps were elevated and viewed. (A) Compact tumor with a few PC-3 cells outside of the tumor border (TB) (drawn in yellow). Arrows indicate individual GFP expressing PC-3 cells. (B) A number of tumor cells ~200 μm beyond the tumor periphery. (C and D) A gradient of metastatic cells extending into the surrounding tissues.

with a few tumor cells outside of the tumor border. Figure 2*B* demonstrates a few tumor cells ~200 μm beyond the tumor peripheri, and Figure 2, *C* and *D*, demonstrates a gradient of metastatic cells extending into the surrounding tissues.

A second method to distinguish between shed genetic material or cells was to determine if shed cells from the s.c. tumors are capable of generating real metastatic lesions. We reasoned that this would be the case if the animals were able to survive long enough for metastatic lesions to appear. To test this concept, *primary* s.c. PC-3^{luc} tumors were established in SCID mice (n = 10). Other animals were implanted with scaffolds only. After 3 weeks, the 1° tumors were resected, and the animals imaged to ensure 1° tumor was removed (Figure 3*A*). The animals were followed for up to 9 months. Two animals became cachectic at 3 months and were sacrificed. On gross dissection, one of these animals had a large abdominal mass (Figure 3*B*) and had disseminated tumors in the lymph nodes, liver (Figure 3*C*), parotid gland, and lungs. The other animal had a large shoulder mass and liver metastases (Figure 3, *D*–*G*). Three additional animals were sacrificed at 6 months, and each had evidence of tumor in multiple organs. One of the three remaining animals was sacrificed at 9 months because the total luciferase signals of the remaining animals began to rise (Figure 3*A*). In one case, a single bone metastasis was noted (Figure 3, *H*–*J*). *Q*PCR demonstrated that tumor cells were present in the remaining two animals after 9 months (not shown). Sham-operated animals did not demonstrate any of these symptoms. These data demonstrate that the disseminated tumor cells from a primary subcutaneous tumor are able to generate metastases as 6 of 8 animals developed tumors.

Tumor Shedding Modulated By Parathyroid Hormone and to Exogenous Tissues

Two further studies were performed to determine the usefulness of our experimental model. In the first set of studies, s.c. tumors were established in SCID mice using PC-3 cells. One group of animals was treated daily with human parathyroid hormone (PTH) beginning 24 hours after tumor implantation for the duration of the study; another group was treated with vehicle only. The levels of PC-3 recovered from a number of tissues were evaluated at 3 weeks. Focusing on the bones, PTH treatments produced variable levels of tumor cells in each of the bone tissues (Figure 4). Most notably, PTH reduced the number of PC-3 cells found in the calvaria and pelvis, while it increased the number of cells in the mandible, tibia, and spine. There were no significant differences noted in the femurs.

Our group has developed an osteogenic assay in which neonatal skeletal elements form bone *in vivo* (e.g., vertebral body or *vossicles*), creating an ectopic bone marrow environment where bone niches are

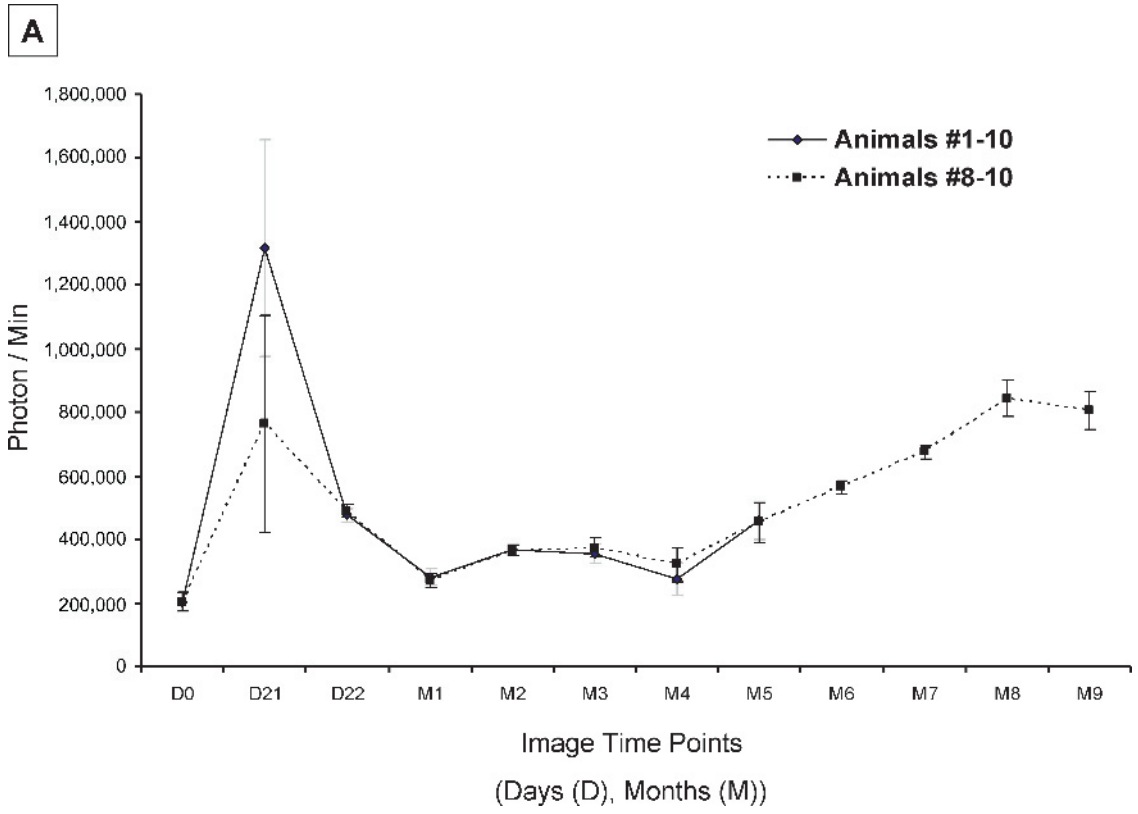

Figure 3. Cells derived from a s.c. tumor generate disseminated tumors over time. Luciferase labeled PC-3− (2×10^5 cells) were implanted s.c. in sponges on the backs of SCID mice (n = 10) as a model of a primary tumor. At 3 weeks, the animals were anesthetized and the tumors resected. (A) Total luciferase signals of animals over the course of 9 months. (B) Abdominal mass (arrows) and (C) liver metastasis (arrows) identified in cachectic animals at 3 months following s.c. tumor implantation and removal. (D and E) Negative and positive (red) immunostaining for pan human cytokeratin (human heart and PCa bone met). Detection of PC-3 cells in a shoulder tumor mass (F) and liver metastasis detected at 3 months (G). Bioluminescent imaging of positive (left arrow) and negative bone (right arrow) metastatic lesions (H) and negative (I) and positive (J) immunostaining for luciferase of the bones shown in H. Scale bars, 100 μm unless indicated.

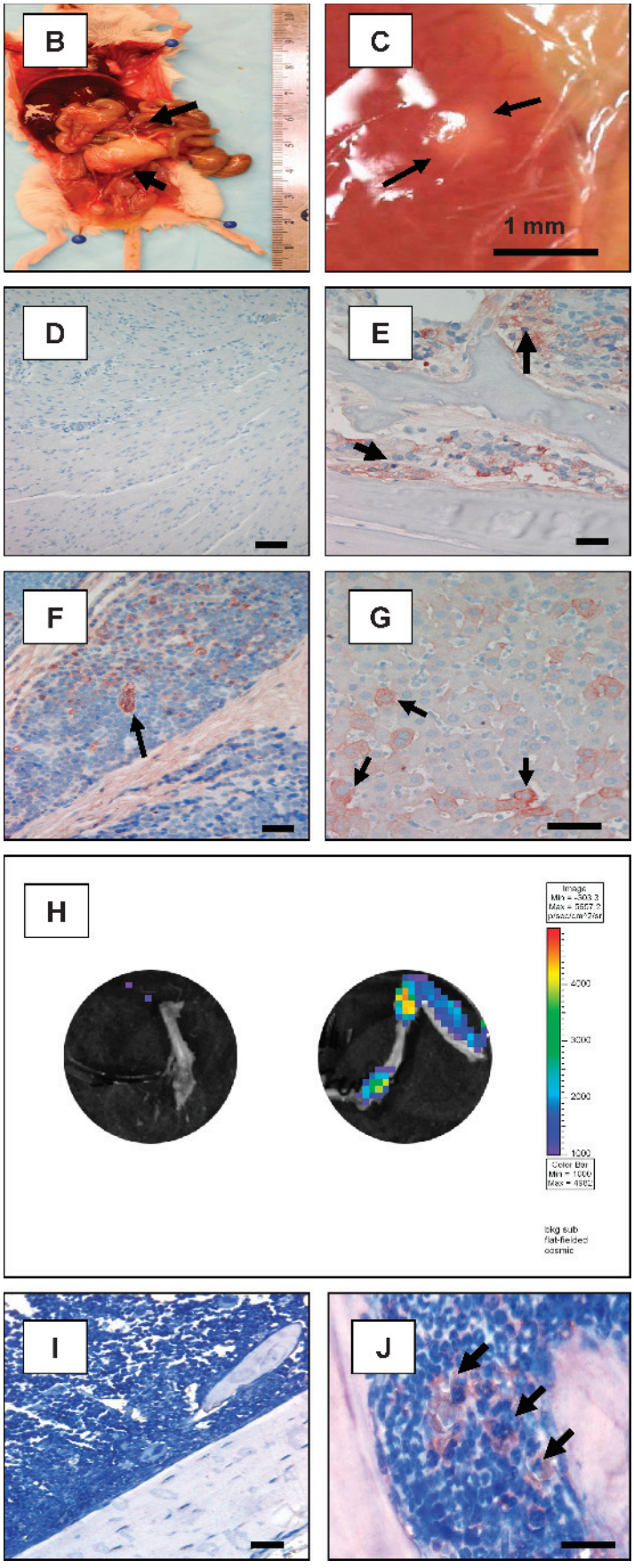

Figure 3. (*continued*)

generated and can be studied [13,14]. We therefore used the metastasis model in conjunction with vossicles to explore if PCa metastasizes to vossicles. Here, mid dorsal s.c. tumors were established using PC-3 cells in SCID mice. At the same time, a total of four vossicles from C57/Bl6 neonates were implanted bilaterally in the right and left shoulder and pelvic regions. At harvest, *Q*PCR was performed. All of the vossicles had tumor cells comparable (or greater) to the levels of tumor cells in the humeri or spine (Figure 5).

Comparisons of Metastasis Generated By Orthotopic Versus *s.c. Tumors*

Recently, debate has centered on the utility of s.c. tumor models *versus* orthotopic models [15–20]. We therefore directly compared the level of tumor dissemination generated by orthotopic *versus* s.c. tumors in our model. Here, 2×10^5 PC-3 cells were either implanted s.c. or directly into the right or left lobe of the dorsolateral prostate. After 3 weeks, the PC-3 cells were identified by *Q*PCR in many tissues, including the bone, for both delivery methods (Figure 6). However, it was clear that for soft-tissue metastases, an orthotopic model was superior. For metastasis in bones, the orthotopic model was also superior, although statistical differences exist.

Discussion

Using an extremely sensitive *Q*PCR assay, we were able to demonstrate that both LNCaP C4-2B and PC-3 cell lines disseminate from a primary s.c. tumor site and populate many distant organs, recapitulating many of the early events necessary for metastasis. This is important for the field as it is critically lacking a metastasis assay in which human tumor cells can be implanted *in vivo* and all the steps of metastasis, including vascular invasion and egress, are achieved.

Our data demonstrate that primary tumors established by LNCaP C4-2B and PC-3 cells shed cells to soft tissues and bone. One surprising aspect of our findings was the observation that different levels of tumor dissemination were noted in a variety of tissues despite the fact that essentially equal levels of LNCaP C4-2B and PC-3 cells were detected in the blood. One possible explanation for these observations may be due to inherent differences in the egress rates of the cells into peripheral tissues once they have reached the vascular compartment. At the present time, little information is available to distinguish between egress rates of tumor cells. Vascular egress constitutes a combination of both vascular adhesion and transendothelial migration. A second scenario may be that equal numbers of cells are seeded into the tissues but that proliferation rates in peripheral tissues vary. Here, combinations of local growth factors and inherent autonomous proliferation differences may have led to different levels of tumor cells in the tissues. Further experimentation will be required to delineate between these possibilities.

Recent debate has centered on the utility of s.c. tumor models *versus* orthotopic models [15–20]. We also share these concerns, and we therefore determined if metastatic cells can be generated from an orthotopic route of tumor initiation. We directly compared orthotopic *versus* s.c. metastasis in our model and determined that the genetic signature of PC-3 cells was identified by *Q*PCR in many tissues, including bone, for both delivery methods. However, it was clear that the orthotopic model was superior for soft tissue metastases. For skeletal metastases, the orthotopic model was superior for the cells shed to the mandible, spine, and tibia. The s.c. method of tumor initiation was superior for cells shed to the calvaria, femur, humeri, and pelvis.

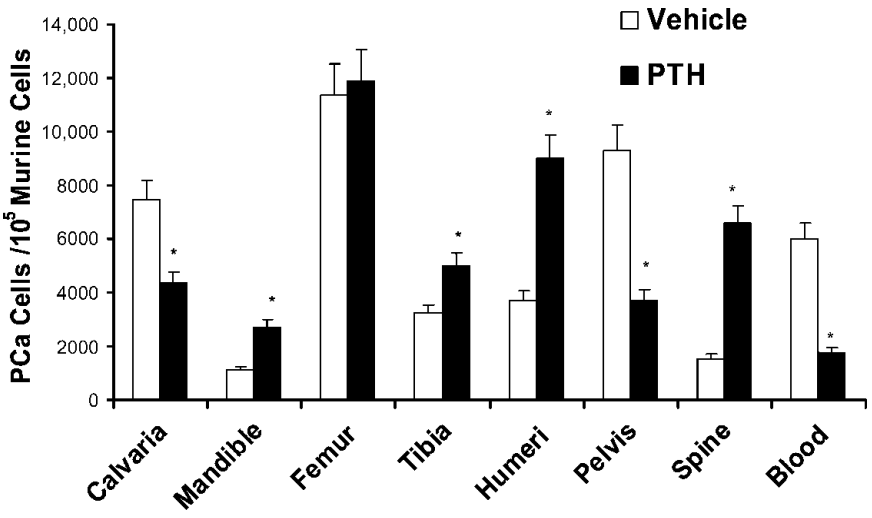

Figure 4. Modulation of tumor dissemination by daily administration of PTH. Subcutaneous tumors were established in SCID mice using PC-3 cells. Mice were injected s.c. with recombinant human PTH fragments 1 to 34 (Bachem) at 40 µg/kg body weight per day or with the vehicle (acidified saline), 7 days/week for 3 weeks ($n = 8$ per group). Body weight was measured weekly, and dose was adjusted accordingly. The levels of PC-3 recovered from a number of tissues were evaluated at 3 weeks. *$P < .05$ from vehicle.

The reason for the differences in seeding to the bones is not clear. A purely vascular rationale relating to blood flow seems unlikely. One possibility is that tumor cells generated at the different primary sites select for cellular populations with different metastatic preference. If this latter prospect is true, it will require further exploration to test this possibility.

As stated in the introduction, a necessary prerequisite for metastasis is having a primary tumor. It is also clear that soluble factors released from a primary lesion are likely to activate distant sites making it more feasible for metastasis to occur. One mechanism that had previously been demonstrated is the activation of vascular endothelial cells to express *de novo* vascular adhesion molecule 1 (VCAM-1) in response to soluble tumor-derived tumor necrosis factor. This facilitates myeloma and osteosarcoma spread through vascular adhesion molecule 1/very late antigen 4 interactions. More recently, it has been demonstrated that the presence of a tumor activates the bone marrow to release endothelial progenitor cells that seed distant organs to establish a premetastatic niche [2–4]. This may influence both the

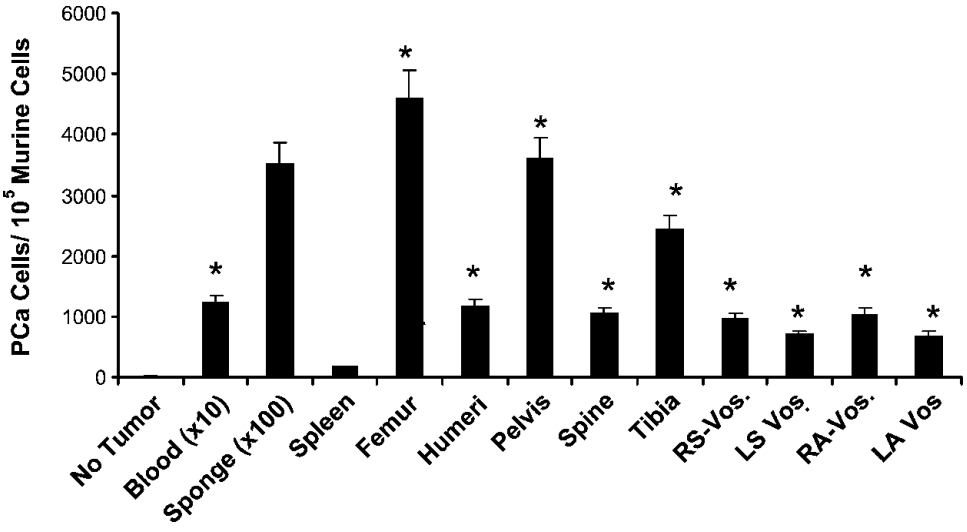

Figure 5. Homing of PCa to vossicle tissues. Lumbar vertebrae (vossicles or Vos.) were isolated from neonatal C57/Bl6 mice within 4 days of birth. Vos. transplants were implanted into s.c. pouches established in the right and left shoulder (RS, LS) or pelvic (RP, LP) pouches into male 5- to 7-week-old SCID mice ($n = 8$). At the same time, s.c. PC-3 tumors were established in sponges in the mid dorsal region. At 3 weeks, the animals were sacrificed, and tissues were removed. *Q*PCR was used to detect human *Alu* sequences derived from the human PCa cells. Resultant numbers were generated against a standard curve established by mixing known numbers of PC-3 in mouse marrow using murine *β-actin* primers. Controls included the femur of sham-operated animals (No Tumor). *Significant differences from the levels of PC-3 in the spleen ($P < .05$). Data show that shed or metastatic PCa cells derived from an s.c. tumor can be identified in the vossicles.

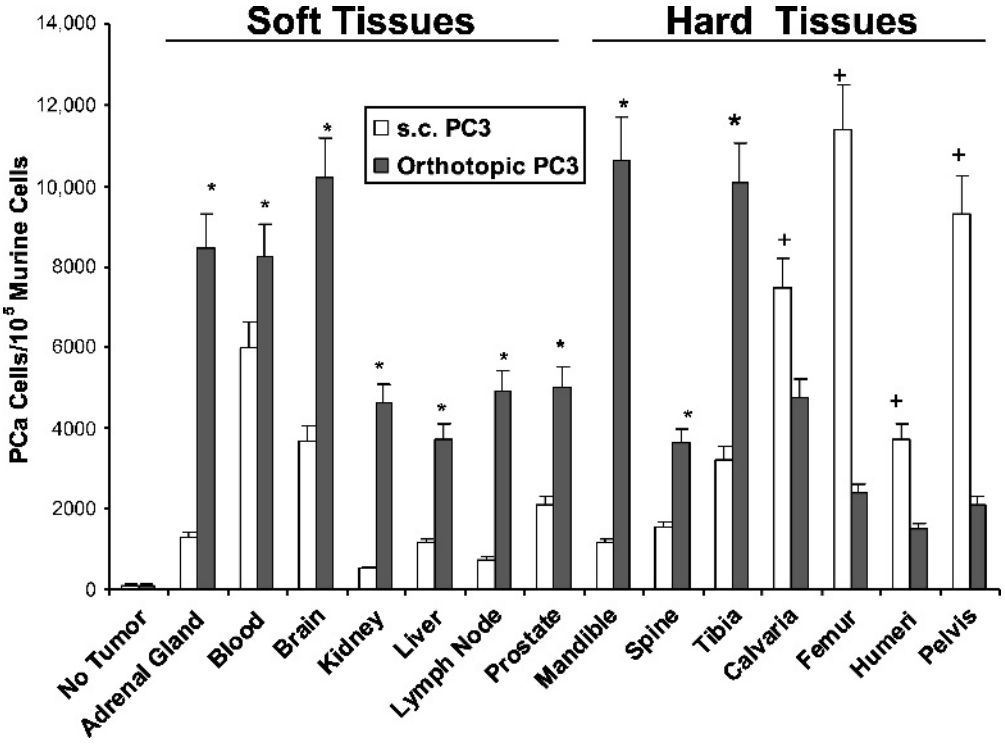

Figure 6. Comparison of metastasis from orthotopic *versus* s.c. sites. Luciferase-labeled PC-3 cells (2×10^5) were implanted s.c. in sponges or orthotopically in SCID mice ($n = 10$) as a model of a primary tumor. At 3 weeks, the animals were sacrificed, and *Q*PCR was used to detect human *Alu* sequences (shown) or luciferase (not shown) derived from the human PCa cells. Human *Alu* sequences were not identified in animals that did not receive a s.c. tumor (No Tumor). *Orthotopic superior to s.c. and $^{+}$s.c. superior to orthotopic ($P < .05$). Data demonstrate that both s.c. and orthotopic routes of establishing a primary tumor results in metastatic seeding of a number of tissues.

seeding rate and/or growth of secondary tumors. It may also precondition selective sites for the distinct metastatic patterns as described by Paget [5] in the original *seed-and-soil* hypothesis.

A particular interest we have in developing this model is its potential flexibility. For example, with PTH injected daily s.c., the observed metastatic patterns were altered. PTH has many known physiologic functions, and PTH-related protein (PTHrP) is produced by virtually all tumor types that metastasize to bone. PTH and PTHrP mediate their major known actions in bone by means of binding to the PTH-1 receptor on osteoblastic cells. Both proteins regulate osteoblast proliferation and differentiation in a time- and dose-dependent manor. Bone remodeling has also been implicated in the localization of tumors to bone. PTH and PTHrP are known to increase bone turnover by enhancing the expression of the receptor activator of NF-κB ligand in osteoblasts, which drives and activates osteoclastic bone resorption. In addition, an emerging role for PTH in the regulation of hematopoiesis has recently been described by expanding the size of the hematopoietic stem cell niche [21–24]. Our data demonstrate that daily PTH injections altered the observed metastastic patterns. One possible mechanism that would account for this finding is the observation that stromal-derived factor 1 (SDF-1) production by osteoblasts is regulated by PTH *in vitro* [23]. When animals were treated with an anabolic regime of PTH for 21 days, significant increases in SDF-1 mRNA expression were observed near the growth plate and epiphysis regions of the long bones [23]. Yet, in serum, immunodetectable SDF-1 levels were significantly reduced (24%) in the PTH-treated animals (vehicle, 408 ± 25 pg/ml SDF-1 *vs* PTH, 308 ± 20 pg/ml SDF-1). Additionally, differential activation of osteoclastic activity can contribute to this possibility. Clearly, further study will be needed to correlate the changes in metastatic cells to SDF-1 levels in each bone. However, these data suggest a possible mechanism for localizing stem cells into a developing marrow where increased expression of SDF-1 in the local marrow environment along with decreased SDF-1 in the serum may create a homing gradient. Yet, the design of our study did not permit us to determine whether these effects were due to the direct effects of PTH on the primary tumor, metastastic spread, or changes in the bone microenvironment.

Another example of the flexibility that this model affords is that we have demonstrated that human PCa cells are able to metastasize to vossicles which could be generated using transgenic tissues [13,14]. This provides a platform to test the effects of different microenvironmental factors on metastasis that would not be possible without first crossing the transgenic animals onto an immunocompromised background. Finally, by resecting the *primary* tumor, the majority of the mice in our study survived longer than 3 months. This strategy, in which animals with disseminated cells survive for relatively long periods of time, may provide opportunities to study issues related to the metastasis-targeted treatments and the induction of tumor dormancy.

Paget [5] first proposed a *seed and soil* metaphor to explain the marked affinity of cancer cells for different tissues stating that, "when a plant goes to seed, its seeds are carried in all directions; but they can only grow if they fall on congenial soil." It is likely that the majority of the cells identified by our PCR methods do not truly represent cells capable of proliferation at distant sites. As such, the model more closely recapitulates the human experience, where a large and perhaps

constant flux of shed tumor cells occurs. Yet clinically, relatively few overt metastatic lesions are observed. It is also likely that cells shed from either the s.c. or orthotopic sites engage the local microenvironments or tissue niches to remain quiescent differently than intravascularly injected cells do. As such, this model may therefore be particularly valuable for identifying mechanisms that regulate quiescence and for identifying prostate cancer stem cells.

References

[1] Fidler IJ (1999). Critical determinants of cancer metastasis: rationale for therapy. *Cancer Chemother Pharmacol* **43** (suppl), S3–S10.

[2] Kaplan RN, Psaila B, and Lyden D (2007). Niche-to-niche migration of bone-marrow–derived cells. *Trends Mol Med* **13**, 72–81.

[3] Kaplan RN, Rafii S, and Lyden D (2006). Preparing the "soil": the premetastatic niche. *Cancer Res* **66**, 11089–11093.

[4] Psaila B, Kaplan RN, Port ER, and Lyden D (2006). Priming the "soil" for breast cancer metastasis: the pre-metastatic niche. *Breast Dis* **26**, 65–74.

[5] Paget S (1889). The distribution of secondary growths in cancer of the breast. *Lancet* **1**, 571–573.

[6] Thalmann GN, Anezinis PE, Chang SM, Zhau HE, Kim EE, Hopwood VL, Pathak S, von Eschenbach AC, and Chung LW (1994). Androgen-independent cancer progression and bone metastasis in the LNCaP model of human prostate cancer [published erratum appears in Cancer Res 1994 Jul 15;54(14):3953]. *Cancer Res* **54**, 2577–2581.

[7] Nyati MK, Symon Z, Kievit E, Dornfeld KJ, Rynkiewicz SD, Ross BD, Rehemtulla A, and Lawrence TS (2002). The potential of 5-fluorocytosine/cytosine deaminase enzyme prodrug gene therapy in an intrahepatic colon cancer model. *Gene Ther* **9**, 844–849.

[8] Replogle-Schwab TS, Getzenberg RH, Donat TL, and Pienta KJ (1996). Effect of organ site on nuclear matrix protein composition. *J Cell Biochem* **62** (1), 132–141.

[9] Rehemtulla A, Stegman LD, Cardozo SJ, Gupta S, Hall DE, Contag CH, and Ross BD (2000). Rapid and quantitative assessment of cancer treatment response using *in vivo* bioluminescence imaging. *Neoplasia* **2**, 491–495.

[10] Kalikin LM, Schneider A, Griffin LB, Dunn RL, Rosol TJ, Shah RB, Rehemtulla A, McCauley LK, and Pienta KJ (2004). *In vivo* visualization of metastatic prostate cancer and quantitation of disease progression in immunocompromised mice. *Cancer Biol Ther* **2**, 656–660.

[11] Lee RH, Hsu SC, Munoz J, Jung JS, Lee NR, Pochampally R, and Prockop DJ (2006). A subset of human rapidly self-renewing marrow stromal cells preferentially engraft in mice. *Blood* **107**, 2153–2161.

[12] Schneider A, Kalikin LM, Mattos AC, Keller ET, Allen MJ, Pienta KJ, and McCauley LK (2005). Bone turnover mediates preferential localization of prostate cancer in the skeleton. *Endocrinology* **146** (4), 1727–1736.

[13] Pettway GJ and McCauley LK (2008). Ossicle and vossicle implant model systems. *Methods in Mol Med* In press.

[14] Koh AJ, Demiralp B, Neiva KG, Hooten J, Nohutcu RM, Shim H, Datta NS, Taichman RS, and McCauley LK (2005). Cells of the osteoclast lineage as mediators of the anabolic actions of parathyroid hormone in bone. *Endocrinology* **146** (11), 4584–4596.

[15] Tsingotjidou AS, Ahluwalia R, Zhang X, Conrad H, and Emmanouilides C (2003). A metastatic human prostate cancer model using intraprostatic implantation of tumor produced by PC-3 neolacZ transfected cells. *Int J Oncol* **23** (6), 1569–1574.

[16] An Z, Wang X, Geller J, Moossa AR, and Hoffman RM (1998). Surgical orthotopic implantation allows high lung and lymph node metastatic expression of human prostate carcinoma cell line PC-3 in nude mice. *Prostate* **34** (3), 169–174.

[17] Rembrink K, Romijn JC, van der Kwast TH, Rubben H, and Schroder FH (1997). Orthotopic implantation of human prostate cancer cell lines: a clinically relevant animal model for metastatic prostate cancer. *Prostate* **31** (3), 168–174.

[18] Stephenson RA, Dinney CP, Gohji K, Ordonez NG, Killion JJ, and Fidler IJ (1992). Metastatic model for human prostate cancer using orthotopic implantation in nude mice. *J Natl Cancer Inst* **84** (12), 951–957.

[19] Langley RR and Fidler IJ (2007). Tumor cell–organ microenvironment interactions in the pathogenesis of cancer metastasis. *Endocr Rev* **28** (3), 297–321.

[20] Talmadge JE, Singh RK, Fidler IJ, and Raz A (2007). Murine models to evaluate novel and conventional therapeutic strategies for cancer. *Am J Pathol* **170** (3), 793–804.

[21] Koh-Paige AJ, Demiralp B, Ealba EL, Mattos A, and McCauley LK (2004). Elucidation of osteoblastic versus bone marrow cellular compartments in the anabolic actions of PTH. *J Back Musculoskeletal Rehabil* **19** (Suppl 1), S17.

[22] Calvi LM, Adams GB, Weibrecht KW, Weber JM, Olson DP, Knight MC, Martin RP, Schipani E, Divieti P, Bringhurst FR, et al. (2003). Osteoblastic cells regulate the haematopoietic stem cell niche. *Nature* **425**, 841–846.

[23] Jung Y, Wang J, Schneider A, Sun YX, Koh-Paige AJ, Osman NI, McCauley LK, and Taichman RS (2006). Regulation of SDF-1 (CXCL12) production by osteoblasts; a possible mechanism for stem cell homing. *Bone* **38**, 497–508.

[24] Zhu J, Garrett R, Jung Y, Zhang Y, Kim N, Wang J, Joe GJ, Hexner E, Choi Y, Taichman RS, et al. (2007). Osteoblasts support B-lymphocyte commitment and differentiation from hematopoietic stem cells. *Blood* **109**, 3706–3712.

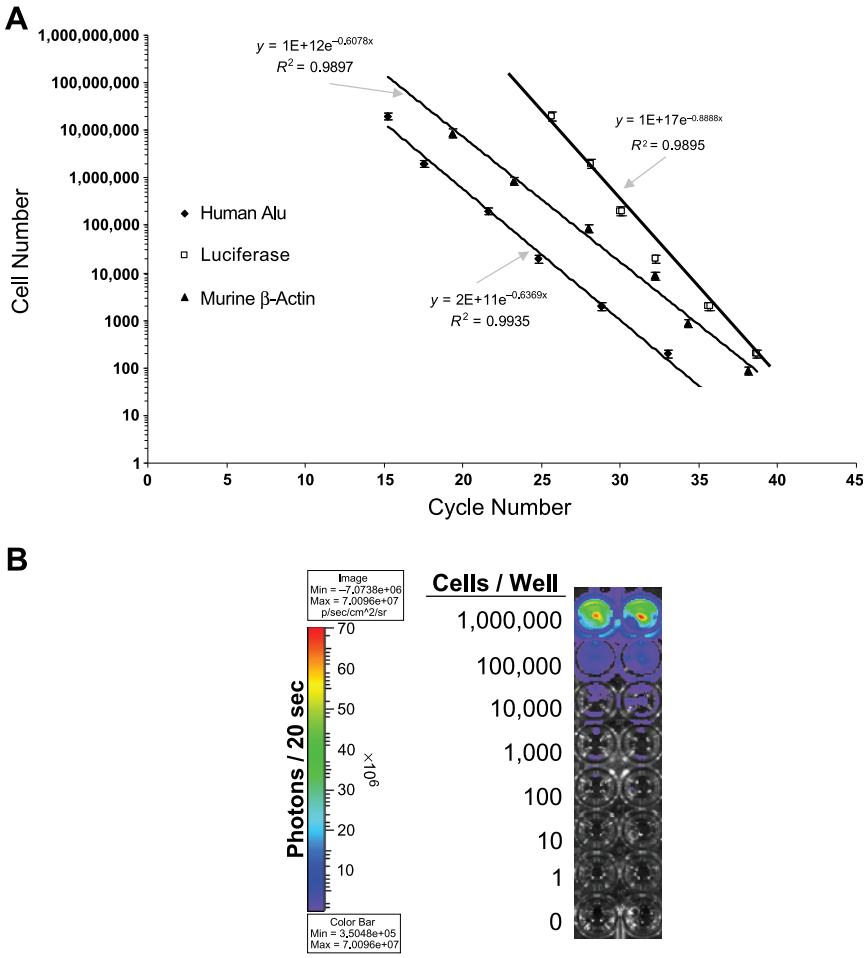

Figure W1. Comparison of the sensitivity of *Q*PCR *versus* bioluminescent imaging (BLI) of PCa cells. Representative standard curves were generated for PC-3^{luciferase} cells. For standard curve generation, log-fold dilution of PC-3^{luciferase} cells (0–1 $\times$ 10^6) mixed with 10^6 nucleated murine bone marrow cells was performed. (A) DNA was extracted, and *Q*PCR was used to determine human *Alu*, luciferase, and murine *β-actin*. PC-3^{luciferase} cell number was plotted against cycle number where *Alu* detection is slightly more sensitive than luciferase detection. (B) BLI of log-fold dilution of PC-3^{luciferase} cells (0–1 $\times$ 10^6) mixed with 10^6 nucleated murine bone marrow cells. Data demonstrate that *Q*PCR is able to detect ~100 cells, whereas the detection limit for the BLI is ~1000 cells.